JOURNAL OF CATALYSIS 46, 37–48 (1977)

Catalytic Oxidation of Carbon Monoxide on Stepped Platinum(111) Surfaces

H. HOPSTER, H. IBACH, AND GEORGE COMSA

Institut für Grenzflächenforschung und Vakuumphysik der Kernforschungsanlage Jülich, 517 Jülich, Germany

Received May 20, 1976

Single-crystal Pt(111) surfaces with a spatially varying step concentration have been prepared. Using Auger spectroscopy the steady-state oxygen coverage and its transient behavior were determined as a function of the O_2 and CO partial pressures. The steady-state coverage was found to depend on the ratio of the partial pressures only. The sticking probability of O_2 and the reaction probability for CO are determined as a function of coverage and step concentration. It was found that the reaction probability is reduced on stepped surfaces. The sticking probability increases exponentially with increasing step concentration and decreases with oxygen coverage. In a model assuming activated adsorption the exponential dependence is linked to the changes in the surface potential due to the presence of steps and adsorbed oxygen atoms. The results show that structural imperfections may have a positive or a negative effect on the CO-oxidation rate depending on the reaction conditions.

1. INTRODUCTION

The important role of steps in the promotion of catalytic reactions has been pointed out by several authors (*1–4*). In those cases where dissociative adsorption of a reactant is rate determining this influence has been attributed to the lowering of the activation barrier for adsorption in the presence of steps. Qualitative observations of electron diffraction patterns (LEED) indicate that this interpretation may also hold for oxygen adsorption on stepped platinum surfaces. Since in the low-pressure regime catalytic oxidation of carbon monoxide proceeds with oxygen preadsorbed at the surface (*5*), a dependence of the oxidation reaction rate on the step concentration is expected. On the other hand, Bonzel and Ku (*5*) have found a relatively high initial sticking coefficient s_0 for the adsorption of oxygen on flat Pt(111) surfaces, leaving little room for a promotion of CO oxidation by steps. Experiments with a supported platinum catalyst (*6*) even show that the specific reaction rate per unit of surface area becomes smaller for smaller crystallites. This suggests that under certain conditions surface roughness may have a negative effect on the reaction.

It is the purpose of this paper to shed some light on this problem. Quantitative relationships between the sticking coefficients, the reaction-rate constants, the oxygen coverage θ, and the step concentration n are established. It is shown that steps lead to a higher or a lower overall yield for a catalytic converter depending on the reaction conditions. This is due to the exponential increase in the sticking coefficient of oxygen with the step concentration n and a decrease in the reaction probability for CO. The large differences in the previously reported sticking coefficients of oxygen may also be explained by this

effect. In addition the results provide experimental evidence that the role of steps on the adsorption kinetics of oxygen may be understood by the model of the collective action of steps (*4*) in which the lowering of the charge transfer barrier due to the reduced work function of a stepped surface is considered. The same model also explains the exponential decrease in the oxygen sticking coefficient with coverage.

2. EXPERIMENTAL

The single-crystal platinum surfaces were prepared from an MRC sample 6 mm in diameter by X-ray orientation and spark erosion cutting. Contrary to conventional surface preparation the surface was given a cylindrical shape by the use of an appropriate erosion electrode. After erosion the surface was gently polished by hand. The orientation of the crystal was such that the center of the crystal had (111) orientation, while surfaces with (11$\bar{1}$) and (100) steps were obtained on the two sides. The crystal was then mounted on a sample holder in a UHV chamber with a capacity for LEED, Auger spectroscopy, mass spectrometry, and separate O_2 and CO gas inlets. The crystal was cleaned by heating at 1100 K in an oxygen atmosphere of 10^{-7} Torr for several hours, followed by flashing to 1700 K. Both calcium and carbon, the main surface contaminants, were removed by this procedure. The residual carbon contamination was less than 1% of a monolayer.

After cleaning, a sharp electron diffraction pattern was observed with the characteristic spot splitting of stepped surfaces (*3*, *7*, *8*). The spacing between the split spots increased from zero to a maximum value when the electron beam was moved across the surface from the center of the crystal to the edges. The maximum spot splitting near the crystal edges corresponded to a step concentration $n \sim 0.12$, where the step concentration n is defined as the ratio of the step atoms to the total number of surface atoms. Since the beam diameters of the LEED and Auger electron sources were ~0.5 and 0.2 mm, respectively, the variations in the step concentration n within the electron beams were sufficiently small (0.02 and 0.008, respectively). The reproducible positioning of LEED and Auger beams on the various crystal locations was obtained by determining the distance between the crystal edge and the measuring position. We could verify the reproducibility of the positioning process by comparing the position of the minimum of the Auger signal in Fig. 3 with the position at which the zero splitting in the LEED pattern was observed. The deviations did not exceed 0.2 mm. The surface coverage with oxygen was measured by a Varian cylindrical mirror Auger analyzer with an integrated electron gun (normal incidence). The diffusion of oxygen atoms across the surface may be neglected. At a temperature of 550 K the diffusion length within 1 hr may be estimated to be $\sim 2.5 \times 10^{-5}$ cm, by taking the adsorption energy of oxygen on platinum 54 kcal/mol and for the activation energy for surface diffusion half this value. At room temperature a rapid carbon buildup was observed with higher beam currents due to the cracking of CO absorbed from the residual gas. Therefore all experiments were carried out at a higher temperature ($T = 550$ K), where the equilibrium coverage θ_{CO} with CO even under ambient pressure is low. The ambient pressure was lower than 2×10^{-10} Torr and the residual CO pressure about 1×10^{-10} Torr or somewhat lower. θ_{CO} may be estimated from the flash desorption temperature of 440 K (*9*) to be roughly $2 \times 10^4\ p_{CO}$ (p_{CO} in Torr). The temperature of 550 K is also approximately the temperature where the maximum reaction rate for carbon monoxide oxidation has been observed (*10*, *11*).

The most difficult problem in the determination of sticking coefficients is the absolute calibration of θ. We have cal-

ibrated our θ scale by measuring the peak-to-peak intensity of the oxygen signal I_O^c of a W(110) surface exposed to 10^{-3} Torr sec of O_2 at higher temperatures and the Pt signal (at 238 eV) I_{Pt}^c of a clean platinum foil in the same system. The total oxygen coverage of the tungsten surface exposed to oxygen under these conditions is $N_W = 1.4 \times 10^{15}$ cm^{-2} (*12*). Assuming the same backscattering factors for W and Pt, the θ calibration is then given by

$$\theta = \frac{I_O}{I_{Pt}} \frac{I_{Pt}^c}{I_O^c} \frac{N_W}{N_{Pt}} = 0.38 \frac{I_O}{I_{Pt}}, \qquad (1)$$

with θ defined as oxygen atoms per platinum surface atoms (N_{Pt}); I_O and I_{Pt} are the peak-to-peak oxygen and platinum signals, respectively, measured on the platinum surface. The factor 0.38 refers to a primary energy of 1500 eV and a modulation voltage of 6 V p–p. The calibration was checked by observing the development of the 2×2 LEED pattern after oxygen adsorption at low temperatures. Sharp fractional order spots were found at I_O/I_{Pt} ratios corresponding to coverages of roughly 0.25 according to the calibration in Eq. (1). Previous authors have assumed that the (2×2)-O LEED pattern corresponds to a coverage of $\theta = 0.5$ (*5*, *13*). However, a coverage of $\theta = 0.25$ is also in agreement with the diffraction pattern (*14*). The previous choice of $\theta = 0.5$ for the (2×2)-O structure was made because it was not understood why the coverage should saturate at rather low values of θ, and because of additional evidence from CO titration experiments (*5*). As has already been shown by Bonzel and Ku (*5*) and by Joebstl (*13*) and will be demonstrated quantitatively in this paper, the low saturation coverage is a result of a low oxygen sticking probability at higher coverages and a high reaction probability with CO (and H_2) present as contaminants in the residual gas. It is therefore assumed that the absolute calibration in Eq. (1) is basically correct, although the error may still be of the order of 20–30%. This error obviously affects the value of the sticking coefficient and the coverage dependence, but not the physical conclusions derived from the data.

In the initial stages of this work an attempt was made to measure the sticking coefficient of oxygen by measuring the oxygen uptake versus exposure. It was realized, however, that every O_2 exposure caused an unintentional rise in the CO partial pressure in the UHV chamber. Although the ratio p_{O_2}/p_{CO} was $\sim$100, the oxygen coverage was still affected by the CO partial pressure, due to the consumption of O adatoms by the CO oxidation reaction. Some effort was made to improve the p_{O_2}/p_{CO} ratio by reducing the pumping speed of the ion pump with a partially closed gate valve and by pumping with a cooled titanium film alone, but with no significant success. It was therefore decided to make use of the oxidation reaction itself in the determination of the sticking coefficient.

As will be shown later, the steady-state oxygen coverage depends on the partial pressure ratio p_{O_2}/p_{CO} alone for a wide range of pressures. The derivative of the oxygen coverage with respect to time may therefore be written as

$$N_{Pt} \frac{d\theta}{dt} = 2s(\theta)\nu_{O_2}p_{O_2} - c(\theta)\nu_{CO}p_{CO}, \qquad (2)$$

where ν_{O_2} and ν_{CO} are the numbers of incident O_2 and CO (in molecules/cm^2·sec·Torr), respectively, and $c(\theta)$ is the reaction probability. If the process were of a simple Rideal–Eley type, $c(\theta)$ would be proportional to θ. $c(\theta)$ describes the probability that a CO molecule hitting the surface reacts with an adsorbed oxygen atom to form a CO_2 molecule. For small coverages c is expected to be proportional to θ.

Four different types of measurements

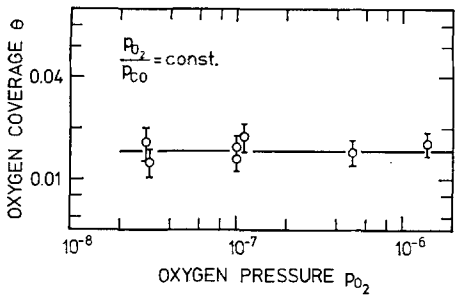

FIG. 1. Steady-state oxygen coverage θ versus oxygen pressure p_{O_2} for a constant partial pressure ratio p_{O_2}/p_{CO_2}.

were performed:

A. The steady-state coverage θ was measured as a function of the ratio p_{O_2}/p_{CO}:

$$\frac{p_{O_2}}{p_{CO}} = \frac{c(\theta)\nu_{CO}}{2s(\theta)\nu_{O_2}}. \tag{3}$$

B. The steady-state oxygen coverage was measured versus step concentration n. (In the following we shall denote by θ_n the oxygen coverage on a surface with a step concentration of n; i.e., θ_0 for the flat surface. The notation θ will be used for the coverage when no specification is necessary.) If $c(\theta_n, n)$ and $s(\theta_n, n)$ denote the reaction probability and sticking coefficients on the stepped surfaces the relation

$$\frac{c(\theta_n, n)}{s(\theta_n, n)} = \frac{c(\theta_0, 0)}{s(\theta_0, 0)} \tag{4}$$

holds for equal p_{O_2}/p_{CO} ratios.

C. For a sudden rise in the oxygen partial pressure Δp_{O_2} the initial slope in θ versus t determines the sticking coefficient

$$N_{Pt}\left.\frac{d\theta}{dt}\right|_{t=0} = 2s(\theta)\nu_{O_2}\Delta p_{O_2}. \tag{5}$$

D. Finally, from a sudden rise in p_{CO} and the initial slope of θ the reaction probability c is measured:

$$N_{Pt}\left.\frac{d\theta}{dt}\right|_{t=0} = -c(\theta)\nu_{CO}\Delta p_{CO}. \tag{6}$$

Three measurements (types A, C, and D) determine two parameters $s(\theta_n, n)$, $c(\theta_n, n)$ each for a certain coverage θ and a certain step concentration n. The consistency of the results may therefore be checked. In addition the functional dependence of c and s on n may be determined from a measurement of type B.

The partial pressures were measured by a quadrupole mass spectrometer calibrated with a nude ion gauge and corrected for the different ionization probabilities of CO and O_2.

3. RESULTS

In Eq. (2) we have implied that the steady-state oxygen coverage θ does not depend on the absolute pressure but on the partial pressure ratio p_{O_2}/p_{CO}. It is seen from Fig. 1 that θ indeed remains constant over two orders of magnitude within the limits of error. The measurements could not be extended to higher pressures as the increasing equilibrium coverage with CO led to a carbon buildup by electron beam cracking. The lower limit of this measurement was set by a competitive reaction with the hydrogen background partial pressure of $\sim 10^{-10}$ Torr. The oxygen coverage versus the partial pressure ratio for the flat and a stepped $[14(111)\times(11\bar{1})]$ surface (i.e., 14 terrace atoms per monoatomic step, or $n = 0.07$) is plotted in Fig. 2. In the low-coverage range, the data points in Fig. 2 are averaged over several individual measurements. The two points marked by crosses are calculated from independent measurements of $c(\theta)$ and $s(\theta)$ according to Eqs. (5) and (6). It is seen that the data are consistent. The results in Fig. 2 show that the steady-state coverage on the stepped surface is higher. This effect is investigated quantitatively when the coverage is measured versus the beam position by moving the crystal perpendicular to the beam (Fig. 3). A linear relation between the coverage and

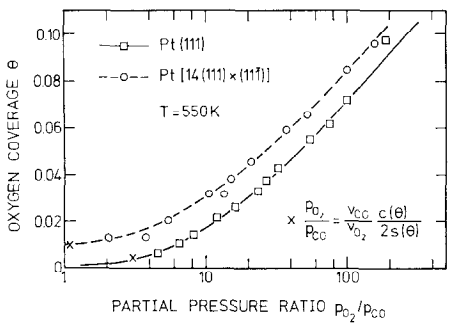

FIG. 2. Steady-state oxygen coverage θ versus partial pressure ratio p_{O_2}/p_{CO} for a flat and a stepped platinum surface. Points marked × are calculated from independent measurements of $c(\theta)$ and $s(\theta)$ (compare Figs. 4 and 5).

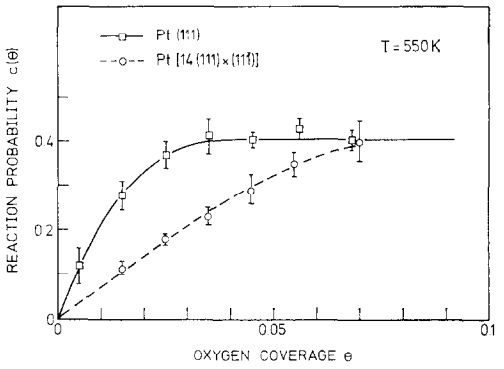

FIG. 4. Reaction probability for a CO molecule $c(\theta)$ versus coverage. The result shows that the reaction mechanism is not of the simple Rideal-Eley type.

the step concentration is found.

$$\theta_n = \theta_0 + \alpha n, \tag{7}$$

where $\alpha \sim 0.24$ except for the surface with (100) steps at the higher ratio p_{O_2}/p_{CO}, in which case α appears to be closer to 0.17. The reaction probability versus θ is plotted in Fig. 4 for both the flat and stepped [14(111) × (11$\bar{1}$)] surfaces. Measurements of the initial slope of $d\theta/dt$ were particularly hampered by the considerable noise in the Auger signal at low coverages. The standard deviation of the individual measurements was $\Delta c = 0.05 - 0.10$. Therefore several individual measurements (5–10) were averaged and the mean values are plotted in Fig. 4. The error bars are the standard deviations of the mean. The results for the sticking coefficients are plotted in Fig. 5. The data points represent individual measurements according to Eq. (5). Again the scattering is due to the noise in the Auger signal. At higher coverages the measurements in Figs. 2 and 4 are more reliable than the direct determination of the sticking coefficient. For $\theta > 0.04$ the full and dotted lines are therefore calculated from $c(\theta)$ (Fig. 4), $\theta = f(p_{O_2}/p_{CO})$ (Fig. 2), and Eq. (3). Below $\theta \sim 0.04$ the solid and

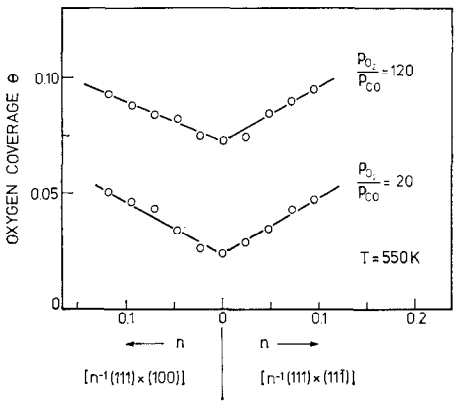

FIG. 3. Steady-state oxygen coverage θ versus step concentration n for two pressure ratios. The linear variation appears to be slightly asymmetric for the two different step orientations for $p_{O_2}/p_{CO} = 120$.

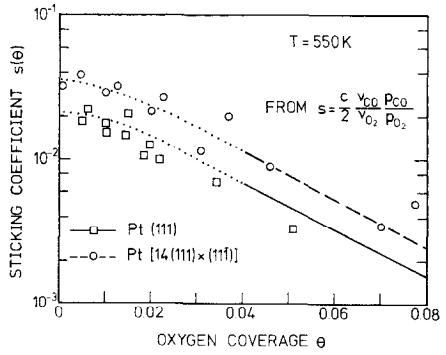

FIG. 5. Sticking coefficient of oxygen $s(\theta)$ versus coverage. For higher coverage $\theta > 0.04$ the lines are calculated from the more reliable data in Figs. 2 and 4 according to Eq. (3) (see text).

dotted lines are drawn to fit the data points starting from the calculated lines for $\theta > 0.04$. The agreement between the values calculated from Figs. 2 and 4 and the coverage of the individual direct measurements of the sticking coefficient illustrates the consistency of the data as well as the use of Eq. (2) for the description of the reaction kinetics.

Except for very low coverages the sticking coefficient decreases exponentially with θ (Fig. 5), in agreement with previous results (*5*). As the two curves in this figure are parallel, one may describe both by

$$s(\theta_n, n) = 0.031 f(n) \exp(-37\theta_n) \quad \text{for} \quad \theta_n > 0.02, \quad (8)$$

where $f(n)$ depends only on the step concentration and has by definition the value $f(0) = 1$ for the flat surface. When surfaces of different step concentration are exposed to the same partial pressure ratio p_{O_2}/p_{CO}, as in the experiment of type B (Fig. 3), Eq. (4) holds and

$$\exp[-37(\theta_n - \theta_0)] f(n) = c(\theta_n, n)/c(\theta_0, 0). \quad (9)$$

Together with Eq. (7), one obtains

$$f(n) = e^{37\alpha n}[c(\theta_n, n)/c(\theta_0, 0)]. \quad (10)$$

The ratio $c(\theta_n, n)/c(\theta_0, 0)$ for $n = 0.07$ and $(11\bar{1})$ steps may be calculated from Figs. 2 and 4 for different partial pressure ratios (Fig. 6). The ratio is approximately 1

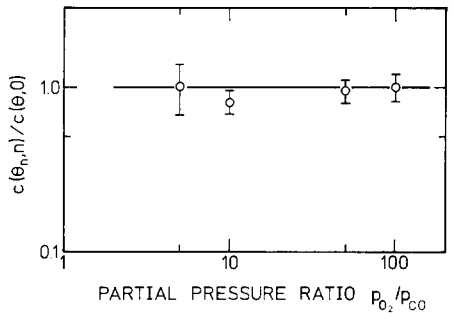

FIG. 6. Ratio of reaction probabilities $c(\theta_n, n)/c(\theta, 0)$ of surfaces exposed to the same partial pressure ratio p_{O_2}/p_{CO}.

and for the following considerations we neglect the deviations. It is further assumed that this holds also for intermediate step concentrations. Then the dependence of the sticking coefficient on the step concentration is

$$f(n) = e^{8.9n} \quad (11)$$

for a Pt$[n^{-1}(111) \times (11\bar{1})]$ surface and an oxygen coverage regime of $0.02 < \theta < 0.10$. The sticking coefficient rises exponentially with the step concentration. The same behavior (with a different exponent) has been found previously with oxygen adsorption on cleaved silicon surfaces (*3*).

As a supplement to these results the work function change connected with the oxygen adsorption was measured by a Kelvin probe (*15*). For a coverage of $\theta = 0.055$, a value of $\Delta\phi = 0.24$ eV was measured.

4. DISCUSSION

4.1. Comparison with Previous Work

It is obvious from the reported data that previous contradictory results of high and low sticking coefficients of oxygen on platinum(111) surfaces can easily be reconciled by assuming various combinations of surface imperfections and partial pressure ratios of O_2 and CO. A smaller or a higher amount of CO is always present as a gas phase contaminant in UHV systems. If its presence is not taken into account the resulting sticking probabilities for oxygen are in error due to the high reaction probability of CO. For instance Weinberg *et al.* (*16*) have calculated the "sticking coefficient" from the oxygen coverage after exposure to 7×10^{-5} Torr for $\tau = 3600$ sec. They found an oxygen coverage of $\theta \sim 0.05$. They also admittedly had a partial pressure of CO of $\sim 1\%$. As seen from Fig. 2, for this partial pressure ratio we have found an equilibrium coverage of $\theta \sim 0.07$, but this equilibrium is in fact reached in about a second at pressures of $\sim 10^{-4}$ Torr.

To calculate a sticking coefficient from

$$s = \theta N_{Pt}/\tau \nu_{O_2} p_{O_2} \qquad (12)$$

as Weinberg *et al.* did is therefore an inadequate procedure, as Bonzel and Ku (*5*) have previously pointed out. In agreement with other authors (*5*), we do not think that high sticking coefficients are a result of carbon contamination. Our upper contamination limit of 1% of a monolayer of carbon throughout the experiments is certainly at least as low as the limit that may be estimated from the Auger spectrum published in the paper of Weinberg *et al.* It is also evident from our data that the categorical statement by Lang *et al.* (*2*) that oxygen is "not adsorbed" on flat (111) surfaces does not hold.

High initial sticking coefficients for O_2 on Pt(111) as well as the exponential dependence of $s(\theta)$ have been reported previously by Bonzel and Ku (*5*), who used the method of CO titration to determine the oxygen coverage. The results differ from ours in two ways:

First, the slope ln s versus θ in Bonzel and Ku's paper is smaller. This is apparently due to a different θ-calibration procedure. Bonzel and Ku have determined the absolute oxygen coverage from the total CO_2 titration yield. This calibration is only as accurate as the determination of the pumping speed. On the basis of this calibration Bonzel and Ku attributed the (2×2)-O LEED pattern to a coverage of $\theta = 0.5$. Thus their calibration seems to differ from ours by a factor of ~ 2, which roughly explains the differences in the slope ln s versus θ (14 and 37, respectively). As the determination of the CO_2 pumping speed may be more uncertain than our Auger calibration for adsorbed oxygen we assume the value reported in this paper to be more reliable.

Second, the work of Bonzel and Ku differs from ours in the absolute value of $s(\theta)$. Our value of s at zero coverage is a factor of 6 lower, which cannot be explained by the different θ calibration. This discrepancy is probably a consequence of the different measuring techniques as well as a difference in crystal perfection. While our sticking coefficient represents the value of a flat (111) surface, the sticking coefficient determined by CO_2 titration represents an average value over the whole surface. The crystal used by Bonzel and Ku had an average misorientation of 1.7° and contained several small angle grain boundaries (*17*); thus the high sticking coefficient observed by Bonzel and Ku may have also been due to the higher residual step density of that surface. Assuming that the difference in the exponents 14 and 37 is caused by calibration, a crystal with an average step concentration of only 0.09 would produce sticking coefficients as observed by Bonzel and Ku. According to Eq. (11) the sticking coefficient of zero coverage should become of the order of 1 if one extrapolates the equation to high step concentration. This is consistent with the high sticking coefficient on the (110) face (*18*), since this face may be considered as composed of a stepped (111) surface with a step concentration of 1.

4.2. The Reaction Probability

As shown in Fig. 4 for a flat platinum-(111) surface the reaction probability saturates at a rather low coverage of 0.03. If the reaction were of a simple Rideal–Eley type, $c(\theta)$ should be proportional to the oxygen coverage. The saturation means that a CO molecule finds its reaction partner even when it strikes the surface at a distance of approximately $\frac{1}{2}(0.03)^{-\frac{1}{2}} \sim 3$ lattice constants from an adsorbed oxygen atom. This is not too surprising. The desorption energy of CO is approximately $E = 1.3$ eV (*9*). Assuming the activation energy for surface diffusion to be roughly one-half of the desorption energy, the diffusion length x within the adsorption

time τ may be estimated from the equations

$$\begin{aligned} x &= (D\tau)^{\frac{1}{2}}, \\ D &= a^2\nu e^{-(E/2kT)}, \\ \tau &= (1/\nu)e^{E/kT}, \\ x &= ae^{E/4kT} \sim 950a, \end{aligned} \tag{13}$$

with ν a frequency factor and a the lattice constant. Although this estimate is rather crude it shows that it is reasonable to assume that the CO molecule may travel quite a distance along the surface before it leaves the surface again by desorption. The reaction probability becomes proportional to θ, below $\theta = 0.03$, which corresponds to an average distance between oxygen atoms of $6a$. This is small compared to the estimated diffusion length of the CO molecules. It appears therefore that the reaction probability for an individual oxygen–carbon monoxide collision on the surface may be rather low. In conception this mechanism is of the Langmuir–Hinshelwood type. In principle one might write the more empirical Eq. (2) in a form reflecting the Langmuir–Hinshelwood mechanism (replacing the second term on the right-hand side by $c\theta_O\theta_{CO}$ and writing a second equation which reflects the variation of θ_{CO}). It can be shown, however, that due to the very short lifetime of the CO molecules on the surface, θ_{CO} follows almost simultaneously the relatively slow variation of θ_O. Moreover, because θ_{CO} is very small under the given experimental conditions it is not accessible to the measurement, and thus no additional information would be gained. On the other hand one may also explain the θ dependence of $c(\theta)$ by a Rideal–Eley mechanism if one assumes that the tails of the interaction potential curves for the chemical reaction CO–$O_{adsorbed}$ extend sufficiently far to attract the impinging CO molecule directly toward its reaction partner.

It seems somewhat surprising that the reaction probability at a given coverage is lower on the stepped surface. One may explain this effect by assuming that the oxygen atoms are more tightly bound in step sites with a Boltzmann distribution between the occupation of terraces and step sites. As the oxygen atoms in step sites may not be available for reaction with the CO, the reaction rate could be reduced unless higher coverages provide enough oxygen atoms on the terrace sites even with the trapped oxygen atoms at the step sites. According to this model a stepped and a flat surface have the same reaction probability when the coverage on the terraces is equal to the coverage on the flat surface. For a partial pressure ratio of, e.g., $p_{O_2}/p_{CO} = 50$, the steady-state coverages are $\theta_{1/14} = 0.065$ and $\theta_0 = 0.052$ for the stepped and flat surfaces, respectively (Fig. 2). The atoms adsorbed on the stepped surface may be adsorbed on the platinum step atoms $N_S = (1/14)N_{Pt}$ (coverage θ_S) and on the terrace atoms $N_T = (13/14)N_{Pt}$ (coverage θ_T). Obviously for the corresponding populations the relation

$$N_{Pt}\theta_{1/14} = N_S\theta_S + N_T\theta_T$$

will hold. This means that the ratio between the terrace and step populations will be

$$\frac{N_T\theta_T}{N_S\theta_S} = \left[\frac{14}{13}\frac{\theta_{1/14}}{\theta_T} - 1\right]^{-1}.$$

As at a given pressure ratio the reaction probabilities for the flat and stepped surfaces are equal (Fig. 6), according to the model we can put $\theta_T = \theta_0$. Thus for the above cases the ratio between the terrace and step populations would be $\sim$2.9. As $N_T/N_S = 13$, an adsorption energy difference between terrace and step sites of

$$\Delta E = -kT \ln (2.9/13) \sim 0.07 \text{ eV} \tag{14}$$

would be required. This is not an unreasonable value as $\Delta E = 0.15$ and 0.25 eV have been measured for hydrogen adsorption on stepped palladium and platinum

surfaces, respectively (*19*, *20*). Further experiments are necessary, however, to decide between the different models.

4.3. Comparison with Conventional Reaction-Rate Constants

In the catalytic literature the question whether a certain reaction is structure sensitive or not is decided by measuring the yield of the desired reaction as a function of the partial pressures for various crystallite sizes in a catalytic reactor. Since the sticking probability of oxygen increases with the step concentration, and the reaction probability decreases, it is not immediately clear whether rough surfaces are an advantage or a disadvantage for the catalytic CO oxidation. It may therefore be useful to consider a simple model reactor and calculate the yield from the atomistic data $s(\theta)$ and $c(\theta)$ as a function of the partial pressures. We define flow rates (in Torr liter sec^{-1}) as $\dot{n}^i_{O_2}$, $\dot{n}^i_{CO}$ and $\dot{n}^f_{O_2}$, $\dot{n}^f_{CO}$, $\dot{n}^f_{CO_2}$ for the input and output streams, respectively, the partial pressures over the catalyst surface p_{O_2}, p_{CO}, p_{CO_2}, and the pumping speed b. Assuming homogeneous partial pressures over the whole catalyst surface one may write the set of continuity equations

$$\dot{n}^i_{O_2} = Fs(\theta)\nu_{O_2}p_{O_2} + \dot{n}^f_{O_2}, \quad (15)$$

$$\dot{n}^i_{CO} = Fc(\theta)\nu_{CO}p_{CO} + \dot{n}^f_{CO}, \quad (16)$$

$$Fc(\theta)\nu_{CO}p_{CO} = \dot{n}^f_{CO_2}, \quad (17)$$

$$\dot{n}^f_x = bp_x \quad \text{for all gases}, \quad (18)$$

with F the surface area of the catalyst. The yield of the reaction defined as

$$y = \dot{n}^f_{CO_2}/\dot{n}^i_{CO} \quad (19)$$

may then be calculated to be

$$y = \left[1 + \frac{b}{c(\theta)F\nu_{CO}}\right]^{-1}. \quad (20)$$

With the steady-state condition (Eq. (3)), $c(\theta)$ may be converted into $c(p_{CO}/p_{O_2})$ with the aid of Figs. 2 and 4. The yield as a function of the partial pressure ratio is plotted in Fig. 7 for a flat (111) surface, a stepped (111) surface, and an ideal catalyst, respectively. Figure 7 illustrates that for oxygen excess the yield is lower on the stepped surface as a result of the smaller reaction probability. For higher CO partial pressures, however, the higher sticking coefficient of oxygen on stepped surfaces becomes the dominating factor. The point of intersection of the yield of flat and stepped surfaces may depend on the step concentration and orientation. The higher reaction rate on flat surfaces for high p_{O_2}/p_{CO} is consistent with the results of McCarthy *et al.* (*6*), who found larger specific reaction rates for crystallite sizes of larger diameter when oxygen was in excess. The same effect has been found for the initial rates in ammonia oxidation (*21*), which indicates that the effect of lower reaction-rate constants on a rough surface may be not specific to the CO system. It is therefore concluded that carbon monoxide

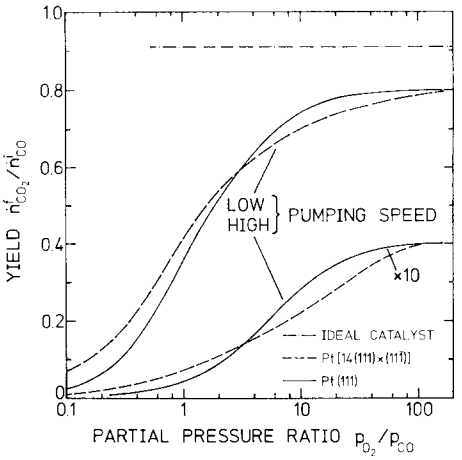

FIG. 7. Yield of a catalytic converter with a flat Pt(111) and a stepped Pt(111) surface as a function of the partial pressure ratio p_{O_2}/p_{CO} for high and low pumping speeds ($b/F\nu_{CO}$ = 10 and 0.1, respectively). The ideal catalyst is defined by $c_{id}(\theta) = 1$ (see the text). The curves for the ideal catalyst coincide when the curve for the high pumping speed is multiplied by 10.

oxidation over platinum is structure sensitive. The effect of roughness may be positive or negative depending on the exact reaction conditions.

Equation (15) was not used for calculating the yield in Eq. (20). However, one should not omit it, because it ensures the necessary oxygen supply. Indeed, from Eq. (15) and the steady-state condition (Eq. (3)) one obtains

$$\dot{n}^i_{O_2} > Fs(\theta)\nu_{O_2}p_{O_2} = \tfrac{1}{2}Fc(\theta)\nu_{CO}p_{CO}. \quad (15a)$$

For real cases the condition is always fulfilled, because by reducing the oxygen input the oxygen coverage is reduced and thus also $c(\theta)$. It seems that a steady state can always be reached. In Fig. 7 we have plotted the yield for an ideal catalyst which we have defined by $c_{id}(\theta) = 1$ (i.e., the reaction probability does not go to zero even when the oxygen coverage vanishes). It is clear that by reducing the oxygen input we will reach

$$\dot{n}^i_{O_2} < \tfrac{1}{2}F\nu_{CO}p_{CO}$$

because in the ideal case also p_{CO} does not depend on the oxygen input. This means that a steady state is no longer possible. This is the reason why in Fig. 7 the yield curve of the ideal catalyst does not continue for values

$$p_{O_2}/p_{CO} < \tfrac{1}{2}(\nu_{CO}/\nu_{O_2}).$$

4.4. The Role of Steps in Adsorption Kinetics

Probably the most interesting result of this work, which may have far-reaching consequences, is the exponential dependence of the sticking coefficient on the step concentration. The same exponential dependence (with a different exponent) has been found with oxygen adsorption on cleaved silicon surfaces (*3*). Since platinum as a *d*-band metal and silicon are chemically rather different it seems that the exponential dependence is a consequence of a general physical principle. In the conventional catalytic literature the role of steps as active sites is considered to be a local effect concentrated on the immediate vicinity of the step sites. Within this model the sticking probability for atoms hitting step sites may be increased. Then, however, the sticking probability referred to the whole surface should be linear in step concentration. The exponential dependence requires a nonlocal model. The fact that steps act nonlocally has already been pointed out by Ibach *et al.* in previous papers (*3*, *4*). It was suggested that the steps lower the activation barrier for dissociative adsorption. A direct measurement of this activation barrier is difficult to perform, however, since the temperature of gaseous oxygen is not variable in conventional UHV systems.

From Eq. (11) one may describe the dependence of the sticking coefficient on the step concentration by

$$f(n) = \exp(0.23 \text{ eV } n/kT), \quad (21)$$

with T the gas temperature.

The lowering of the activation barrier for dissociative adsorption and thus the increase of the sticking coefficient has been correlated (*4*) with the lowering of the work function of stepped surfaces (*22*). A smaller work function should make the charge transfer from the solid to the electronegative oxygen atoms easier. Considering model potentials for molecular and atomic oxygen and assuming that the change in the electron potential in the relevant reaction distance is equivalent to the change in the work function $\Delta\phi$, the relation

$$\Delta E_a = \rho\Delta\phi \quad (22)$$

has been derived with ρ of the order of 0.5 depending on the potential parameters, where ΔE_a is the change of the activation barrier for dissociative adsorption.

For a quantitative evaluation of the model, $\Delta\phi$ should be replaced by the change of the potential of an electron relative to the Fermi level in the distance from the surface

where the activation barrier lies. For stepped surfaces this potential is difficult to estimate as the electron charge distribution is not known.

The estimation of $\Delta\phi$, however, is possible in the case of oxygen adsorption. The decrease in the sticking coefficient with oxygen coverage can also be explained by the influence of the electron potential on the activation barrier. As the work function rises with oxygen coverage the model predicts the sign and the exponential dependence correctly. The potential at the reaction distance d may be calculated assuming point dipole potentials for the adsorbed oxygen atoms.

$$\Delta\phi(d) = \frac{pd}{4\pi\epsilon_0} \sum_n \frac{1}{r_n^3}, \qquad n = (n_1, n_2), \quad (23)$$

where p is the dipole moment and r_n the distance from an oxygen atom. The dipole moment may be calculated from the observed work function change

$$p = \epsilon_0(\Delta\phi/\theta N_{Pt}), \quad (24)$$

where $\Delta\phi/\theta$ is roughly constant for small θ. Since r_n scales with $\theta^{-\frac{1}{2}}$ the potential $\Delta\phi(d)$ is proportional $\theta^{\frac{3}{2}}$ (i.e., $\Delta Ea = A\theta^{\frac{3}{2}}$). The model therefore predicts for the sticking coefficient

$$s = s_0 \exp[-(\Delta E_a/kT)] = s_0 \exp[-(A\theta^{\frac{3}{2}}/kT)]. \quad (25)$$

A plot of ln s versus $\theta^{\frac{3}{2}}$ is shown in Fig. 8. As in Fig. 5 the lines are calculated from the results in Figs. 2 and 4 for coverages $\theta > 0.04$. The data points represent the individual measurements as in Fig. 5. It is seen that the plot in Fig. 8 gives a much better fit to a straight line than a plot of ln s versus θ. In making this comparison one has to bear in mind the comments made in Section 3 concerning Fig. 5: The solid and the dotted lines for $\theta > 0.04$ were calculated from $c(\theta)$ (Fig. 4), $\theta = f(p_{O_2}/p_{CO})$ (Fig. 2), and Eq. (3), because these data are more reliable for these higher coverages

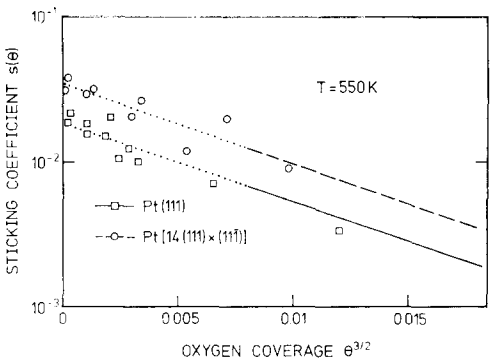

FIG. 8. Sticking coefficient of oxygen $s(\theta)$ versus $\theta^{\frac{3}{2}}$. As in Fig. 5 the data points represent individual measurements according to Eq. (5), while for $\theta^{\frac{3}{2}} > 0.008$ the solid and dotted lines are calculated from the more reliable data presented in Figs. 2 and 4 according to Eq. (3) (see text).

than the direct measurement of the sticking coefficient. Evidently the same applies for Fig. 8. We think that the better fit in Fig. 8 supports the model of the influence of electrostatic potentials on the activation barrier.

Further confirmation is obtained from an estimate of the prefactor A by means of Eqs. (22) and (23). For this purpose we assume a regular hexagonal surface lattice of the oxygen atoms with a lattice constant a. The area of the unit cell is then

$$F = \tfrac{1}{2}\sqrt{3}a^2 = (\theta N_{Pt})^{-1}. \quad (26)$$

Then Eq. (23) becomes

$$\Delta\phi(d) = \frac{pd}{4\pi\epsilon_0} 0.81(\theta N_{Pt})^{\frac{3}{2}} \sum_n \frac{1}{n^3}. \quad (27)$$

The minimum potential and therefore the smallest enhancement of the activation barrier occurs in the center of a unit mesh. The lattice sum in Eq. (27) is then $\sim$26. With the measured work function change and $d \sim 2.5$ Å, Eq. (27) becomes

$$\Delta\phi(d) \sim 7.2 \text{ eV } \theta^{\frac{3}{2}}. \quad (28)$$

From Eq. (22), ΔE_a may then be estimated to be roughly $\sim$3.6 eV $\theta^{\frac{3}{2}}$. The straight

line in Fig. 8 corresponds to

$$s = 0.018 \exp\left[-(3.2 \text{ eV } \theta^{\frac{3}{2}}/kT)\right]. \quad (29)$$

The model of the influence of the electrostatic potential on the activation barrier therefore predicts correctly the sign of the effect, the exponential dependence, and, approximately, the exponent.

CONCLUSION

The method of observing the oxidation reaction of CO by measuring the local oxygen concentration on a cylindrically shaped platinum single crystal as a function of partial pressure ratios and as a function of time provides a rather complete set of data on the sticking coefficient, the reaction probability, and their dependence on structural defects. It was shown that surface steps have opposite effects on the sticking coefficient of oxygen and on the reaction probability. Steps therefore have a positive or a negative effect on the reaction rate depending on the exact reaction conditions. In any case CO oxidation on platinum has to be considered as "primary structure sensitive" (*23*). The regime of pressure ratios of the reactants where the positive or the negative effect prevails probably also depends on the nature of the structural defects. In conventional catalytic experiments with (apart from the crystal size) unspecified catalysts, oxidation rates per surface area may appear as positively, negatively, or not at all influenced by the size of the crystallites. This may provide a basis for the solution of apparent contradictions in previous experimental results.

ACKNOWLEDGMENTS

The experiments were performed in an apparatus planned and built by S. Berger and K. Besocke. We would like to acknowledge their considerable experimental support. In addition, one of us (H. Hopster) is very indebted to K. Besocke for introducing him to UHV technology as well as to the other experimental procedures. The very helpful discussions with H. P. Bonzel and H. Wagner are also acknowledged.

REFERENCES

1. Perdereau, J., and Rhead, G. E., *Surface Sci.* **24**, 555 (1971).
2. Lang, B., Joyner, R. W., and Somorjai, G. A., *Surface Sci.* **30**, 454 (1972).
3. Ibach, H., Horn, K., Lüth, H., and Dorn, R., *Surface Sci.* **38**, 433 (1973).
4. Ibach, H., *Surface Sci.* **53**, 444 (1975).
5. Bonzel, H. P., and Ku, R., *Surface Sci.* **40**, 85 (1973).
6. McCarthy, E., Zahradnik, J., Kuczynski, G. C., and Carberry, J. J., *J. Catal.* **39**, 29 (1975).
7. Henzler, M., *Surface Sci.* **19**, 159 (1970).
8. Besocke, K., and Wagner, H., *Surface Sci.* **52**, 653 (1975).
9. Morgan, A. E., and Somorjai, G. A., *J. Chem. Phys.* **51**, 3309 (1969).
10. Bonzel, H. P., and Ku, R., *J. Vac. Sci. Technol.* **9**, 663 (1972).
11. Palmer, R. L., and Smith, J. N., *J. Chem. Phys.* **60**, 1453 (1974).
12. Engel, T., Niehus, H., and Bauer, E., *Surface Sci.* **52**, 237 (1975); and to be published.
13. Joebstl, J. A., *J. Vac. Sci. Technol.* **12**, 347 (1975).
14. Tucker, C. W., *J. Appl. Phys.* **35**, 1897 (1964).
15. Berger, S., and Besocke, K., *Rev. Sci. Instrum.* **47**, 840 (1976).
16. Weinberg, W. H., Lambert, R. M., Comrie, C. M., and Linnett, J. W., *in* "Proceedings of the Fifth International Congress on Catalysis" (J. W. Hightower, Ed.), pp. 33-519. North-Holland, Amsterdam 1973.
17. Bonzel, H. P., private communication.
18. Ducros, R., and Merrill, R. P., *Surface Sci.* **55**, 227 (1976).
19. Conrad, H., Ertl, G., and Latta, E. E., *Surface Sci.* **41**, 435 (1974).
20. Christman, K., Ertl, G., and Pignet, T., *Surface Sci.* **54**, 365 (1976).
21. Ostermeier, J. J., Katzer, J. R., and Manogue, W. H., *J. Catal.* **33**, 457 (1974).
22. Besocke, K., and Wagner, H., *Surface Sci.* **53**, 351 (1975); *Phys. Rev. B* **8**, 4597 (1973).
23. Manogue, W. H., and Katzer, J. R., *J. Catal.* **32**, 166 (1974).